

Comprehensive Antibody Epitope Mapping of the Nucleocapsid Protein of Severe Acute Respiratory Syndrome (SARS) Coronavirus: Insight into the Humoral Immunity of SARS

YUNFEI LIANG,¹ YING WAN,¹ LI-WEN QIU,² JINGRAN ZHOU,¹ BING NI,¹ BO GUO,¹ QIANG ZOU,¹ LIYUN ZOU,¹ WEI ZHOU,¹ ZHENGCAI JIA,¹ XIAO-YAN CHE,^{2*} and YUZHANG WU^{1*}

Background: The epidemic outbreak of severe acute respiratory syndrome (SARS) posed a worldwide threat to public health and economic stability. Although the pandemic has been contained, concerns over its recurrence remain. It is essential to identify specific diagnostic agents and antiviral vaccine candidates to fight this highly contagious disease.

Methods: We generated 14 monoclonal antibodies (mAbs) specific to the SARS coronavirus (SARS-CoV) nucleocapsid (N) protein and used these to thoroughly map the N protein antigenic determinants. We identified the immunodominant antigenic sites responsible for the antibodies in sera from SARS patients and antisera from small animals and differentiated the linear from the conformational antibody-combining sites comprising the natural epitopes by use of yeast surface display.

Results: We identified 5 conformational and 3 linear epitopes within the entire N protein; 3 conformational and 3 linear epitopes were immunodominant. The antibody responses to the N protein fragments in mammalian sera revealed that 3 regions of the N protein are strong antigenic domains. We expanded the specificity of the N protein epitope and identified 4 novel confor-

mational epitopes (amino acids 1–69, 68–213, 212–341, and 337–422).

Conclusion: The antigenic structures identified for the SARS-CoV N protein, the epitope-specific mAbs, and the serum antibody profile in SARS patients have potential use in the clinical diagnosis and understanding of the protective immunity to SARS-CoV.

© 2005 American Association for Clinical Chemistry

Atypical pneumonia caused by the severe acute respiratory syndrome coronavirus (SARS-CoV)³ (1–4) has spread through 30 countries on 6 continents since late 2002. Although many of the clinical and epidemiologic features of SARS remain to be elucidated, hematologic (5, 6) and serologic (7–9) data suggest that IgG seroconversion plays a key role in virus growth inhibition and disease prognosis. Serodiagnosis and serosurveillance of SARS (10, 11) have revealed that nucleocapsid (N) protein-specific antibodies in the serum of SARS patients have higher sensitivity (12–14) and longer persistence (9) than those of other structural proteins of SARS-CoV. This finding has led to the current focus on potential targets for antiviral therapy.

The N proteins of other coronaviruses shed more antigen than other structural proteins in infected cells (15) and are among the most immunoreactive viral proteins. N-protein-specific monoclonal antibodies (mAbs) have a protective effect in mice after lethal virus challenge (16, 17), and immunization with the N protein of the

¹ The Institute of Immunology, PLA, The Third Military Medical University, Shapingba District, Chongqing, China.

² Central Laboratory, Zhujiang Hospital, The Southern Medical University, Guangzhou, China.

*Address correspondence to Yuzhang Wu at: The Institute of Immunology, PLA, The Third Military Medical University, Shapingba District, Chongqing 400038, People's Republic of China; fax 086-023-68752789; e-mail wuyuzhang@gmail.com; or Xiao-yan Che at: Central Laboratory, Zhujiang Hospital, The Southern Medical University, Guangzhou 510282, People's Republic of China; fax 086-020-61643592; e-mail linche@pub.guangzhou.gd.cn.

Received March 14, 2005; accepted May 26, 2005.

Previously published online at DOI: 10.1373/clinchem.2005.051045

³ Nonstandard abbreviations: SARS, severe acute respiratory syndrome; CoV, coronavirus; N, nucleocapsid; mAb, monoclonal antibody; IFA, immunofluorescence assay; GST, glutathione S-transferase; PBS, phosphate-buffered saline; FITC, fluorescein isothiocyanate; and RAYS, recombinant antigen expression on yeast surface.

avian infectious bronchitis coronavirus induces an immune response that protects chickens from infection by this virus (18,19). These findings suggest that the N protein of the SARS-CoV, or its fragments, is an efficacious immunoprotective antigen (20). Determination of the antigenic structure of the viral protein may lead to identification of the epitope responsible for the harmful vs beneficial effects on humoral immunity and provide valuable information for SARS vaccine development.

To characterize the immunogenicity and immunoreactivity of the SARS-CoV N protein and potential antigenic sites, several groups have used synthetic peptides (21–24) and protein microarrays (25) to analyze sera from SARS patients. The antigenic sites on the N protein of SARS-CoV identified in these studies were limited to strong immunodominant antigenic sites because few antibodies in the sera from SARS patients recognized the less effective immunogenic determinants, which are usually obscured by the more numerous antibodies to stronger immunodominant determinants (26). The identified antigenic sites were mainly linear epitopes (27). The antigenic structure and the precise locations of epitopes on the SARS-CoV N protein are still unknown because of the absence of proteins expressed by the eukaryotic system and of N-protein-specific mAbs that would enable characterization of the antigenic structure in the context of antigen-antibody interaction.

To precisely map the epitopes of the SARS-CoV N protein, it is necessary to optimize the production of the N protein and its fragments as they occur in nature, along with N-protein-specific mAbs. We generated 14 SARS-CoV N-protein-specific mAbs and used these for epitope mapping, thus identifying a range of epitopes and the immunodominant antigenic structures of the SARS-CoV N protein.

Materials and Methods

VIRUSES AND CELLS

The SARS-CoV strain GD01 (GenBank accession no. AY278489), isolated from patients with atypical pneumonia in Guangdong Province, was the viral source and was cultured in Vero cell lines (CCL-81; ATCC). The human coronavirus strains 229E (VR740; ATCC) and OC43 (VR759; ATCC) were propagated in MRC-5 cells (CCL-171; ATCC) and BS-C-1 cells (CCL-26; ATCC), respectively. All cell lines were cultured in DMEM growth medium supplemented with 100 mL/L fetal bovine serum (Gibco Invitrogen) at 37 °C in 5% CO₂. All experiments with SARS-CoV were performed in a biosafety level 3 laboratory.

SERUM SPECIMENS

Forty-seven serum specimens were collected from convalescent SARS patients in 4 different hospitals in Beijing and Guangzhou Province, China. All patients were classified according to the SARS clinical diagnostic criteria released by the WHO. Of the 47 serum samples, those

from 20 adult males and 20 adult females were serologically confirmed by an immunofluorescence assay (IFA) and ELISA, as described previously (28). Serum samples collected in 2003 from 40 healthy blood donors and 38 patients with upper respiratory symptoms but not infected with the SARS virus were used as controls.

GENERATION AND SCREENING OF SARS-CoV N-PROTEIN-SPECIFIC HYBRIDOMA CELL LINES

Construction of recombinant SARS-CoV N protein and immunization procedures were performed as described previously (28,29). In brief, the cDNA gene encoding the SARS-CoV N protein was extracted from the filtered supernatants of SARS-CoV-infected Vero cells by use of the QIAamp Viral RNA Mini Kit (Qiagen). The sequence coding for the SARS-CoV N protein was then cloned into the pGEX-5X-3 vector (Pharmacia Biotech) in frame and downstream of the glutathione *S*-transferase (GST)-encoding sequence. The GST-N fusion protein was expressed and purified with a GST Gene Fusion System (Pharmacia Biotech). HPLC analysis showed that the purity of this purified N fusion protein was >95%. The recombinant N fusion protein was detected by Western blot analysis with sera of convalescent-phase SARS patients as the primary antibody. A SARS-CoV-infected cell culture filtrate was used as a positive control. Horseradish peroxidase-labeled goat anti-human IgG was used as the secondary antibody. Aminoethyl carbazole Single Solution chromogen (Zymed Laboratories) was used for signal detection. The concentration of purified recombinant N fusion protein was determined by the Coomassie Plus protein assay (Pierce Biotechnology).

Six-week-old female BALB/c mice were immunized with the purified recombinant N protein mixed with an equal volume of monophosphoryl lipid A and trehalose dicorynomycolate (MPL+TDM) adjuvant (Sigma). Splenocytes from the immunized mice were fused with NS-1 myeloma cells. The fused hybridoma cells were propagated in RPMI 1640 supplemented with 100 mL/L fetal bovine serum, hypoxanthine, aminopterin, and thymidine. The culture supernatants of the hybridoma cells were screened for antibody production by indirect ELISA. The coating antigens used were recombinant GST (Pharmacia Biotech), recombinant GST-N protein, and virus-cell lysates of the SARS-CoV. Hybridoma clones that reacted with the GST-N protein and virus-cell lysates but not with GST were selected and subcloned twice by limiting dilution. Fusion of splenocytes from mice immunized with NS-1 myeloma cells produced more than 100 positive hybridoma lines, of which 14 cell lines were selected on the basis of their strong reactivity with the N protein as shown by ELISA. The cell lines were then frozen and stored in liquid nitrogen. The classes and subclasses of the 14 mAbs were determined by use of the Mouse Monoclonal Antibody Isotyping Kit (Roche Applied Science) according to the manufacturer's instructions.

PRODUCTION AND PURIFICATION OF mAbs

To produce mAb-containing ascites fluid, fourteen 6-week-old female, specific pathogen-free BALB/c mice were given 1-mL intraperitoneal injections of pristane 1 week before inoculation with 2.5×10^6 mAb-producing hybridoma cells. Two weeks later, harvested ascites samples were examined for their anti-SARS-CoV N protein specificity by an ELISA as described above. mAbs were purified by protein G column chromatography (Pharmacia Biotech) according to the manufacturer's instructions.

WESTERN BLOT ANALYSIS

The purified SARS-CoV N proteins were separated by sodium dodecyl sulfate–polyacrylamide gel electrophoresis and transferred to polyvinylidene fluoride membranes. The membranes were then blocked in Tris-buffered saline (150 mmol/L NaCl, 50 mmol/L Bis-Tris, pH 7.5) containing 0.5 mL/L Triton X-100 and 50 g/L nonfat milk for 2 h at room temperature and then incubated with purified mAbs for 2 h. After a wash with Tris-buffered saline–Triton, the membranes were incubated with the goat anti-mouse IgG–peroxidase conjugate. Aminoethyl carbazole chromogen was used for signal detection.

IFA

Vero cells infected with SARS-CoV, MRC-5 cells infected with human CoV 229E, and BS-C-1 cells infected with human CoV OC43 were first harvested and then washed twice in ice-cold phosphate-buffered saline (PBS). The cells were deposited on 8- to 10-well chamber slides, air-dried, and fixed in acetone. After a wash with PBS, the slides were incubated with purified mAbs at 37 °C for 1 h and incubated with fluorescein isothiocyanate (FITC)–conjugated goat anti-mouse IgG at 37 °C for 30 min. The slides were stained with 0.25 g/L Evans blue in PBS and analyzed with a Leica Eclipse epifluorescence microscope.

PREPARATION OF N-PROTEIN–SPECIFIC ANTISERA

For vaccination, four 6-week-old female BALB/c mice were immunized intradermally with 100 μ g of purified recombinant N protein in complete Freund's adjuvant emulsion (Sigma) for the first injection on day 0. Equal-quality immunogen mixed with incomplete Freund's adjuvant was used for the booster injections on days 7, 14, 21, and 28. Antisera were collected 4 days after the final inoculation. The anti-N-protein antibody responses of the antisera were tested by ELISA using the purified N protein as the coating antigen.

SEQUENCE ANALYSIS AND EPITOPE PREDICTION

The amino acid sequence encoding for the complete N protein was derived from SwissProt/TrEMBL (accession no. P59595). To analyze the molecular characteristics and structural information of the SARS-CoV N protein, we

used the bioinformatics servers on the Internet, including the ProtScale server (Swiss Institute of Bioinformatics), JPred2 server (University of Dundee School of Life Sciences), and the PredictProtein server (Columbia University Bioinformatics Center), and DNASTAR software (DNASTAR, Inc.). The predicted results are shown in Fig. 1A. On the basis of the predicted antigenic locations, putative epitopes within the N protein were referred for further plasmid construction.

CONSTRUCTION OF YEAST EUKARYOTIC EXPRESSION PLASMIDS

To construct the yeast expression vectors, a panel of series-truncated and nested-deletion mutations was designed according to the results of sequence analysis and epitope predictions (Fig. 1B). Reverse transcription-PCR was performed with the forward primer 5'-CGGAATTCATGTCTGATAATGGACCCCAA-3', the reverse primer 5'-CGTCTAGATTATGCCTGAGTTGAATCAGCA-3', and the SARS-CoV RNA template described above. The restriction enzymes were purchased from New England Biolabs, and the pYD1 Yeast Display Vector Kit was from Invitrogen. The sequence coding the complete N protein was digested with *EcoRI* and *XbaI*, ligated into the pcDNA3.1 vector (Invitrogen), which digested with the same restriction enzymes produced the pcDNA3.1-N plasmid. To obtain the pYD1-N yeast expression plasmid, the full length of the N gene from the pcDNA3.1-N plasmid was excised with *EcoRI* and *ApaI* and then ligated into pYD1. To produce series-truncated and nested-deletion mutations, 2 linkers (linker 1, *EcoRI*, *XhoI*, *HindIII*, *NheI*, *EagI*, *HindIII*; linker 2, *EcoRI*, *NheI*, *BstXI*, *XbaI*, *EagI*, *HindIII*) were designed using Vector NTI 7.0.0 software (Informax, Inc.), synthesized (Sangon Co. Ltd.), and then cloned into the pMD18-T vector (Takara Co., Ltd.). A panel of N gene segments was subcloned into the pMD18-T linker 1 and pMD18-T linker 2 plasmids. The N gene segments were digested with *EcoRI* and *EagI* enzymes and then subcloned into the pYD1 expression vector. All constructed plasmids were identified by enzyme digestion and confirmed by sequencing (Takara Co.). After transformation into the *Escherichia coli* strain XL1-blue and plasmid extraction, the pYD1 plasmids containing the full-length N gene and the various N gene fragments (Fig. 1B) were prepared for yeast transformation and induction of protein fusion.

YEAST TRANSFORMATION

The reagents used in this experiment were purchased from Sigma-Aldrich. The lithium acetate method was used for yeast transformation. Briefly, the glycerol stock of EBY100 was streaked out on a minimal dextrose plate containing leucine and tryptophan and then incubated at 30 °C until colonies appeared 2 days later. The EBY100-competent cells were prepared with lithium acetate (1.0 mol/L), salmon sperm DNA (50 μ g), and polyethylene

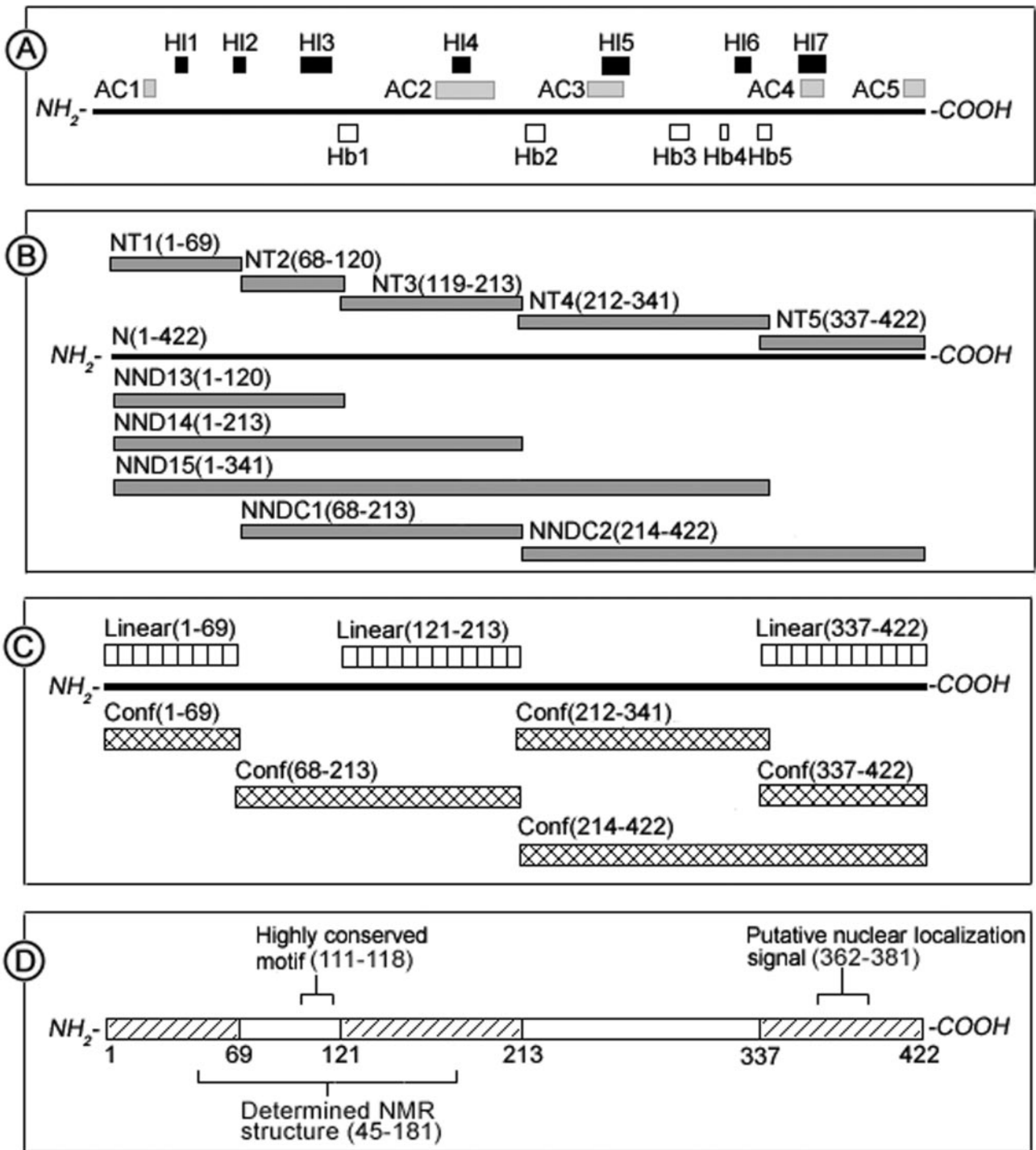


Fig. 1. Schematic illustration of epitope prediction, yeast expression plasmid construction, and antibody epitope mapping of the SARS-CoV N protein.

(A), *Hi1* to *-6*, *Hb1* to *-6*, and *AC1* to *-5* indicate the most hydrophilic regions, hydrophobic regions, and accessible residues of the N protein, respectively. (B), the black bar represents the full-length N protein, and the gray bars represent the N protein fragments that were cloned into the yeast expression vector pYD1 plasmid. The symbols above each bar show the names of the fusion proteins, and the amino acid numbers of the start and stop positions on the N protein are indicated in parentheses. (C), linear and conformational (*Conf*) epitopes located in the regions of the N protein identified in this study. (D), the strong antigenic domains of the N protein are indicated by hatched regions in the horizontal bar.

glycol (500 g/L) admixtures, and transformed with pYD1, pYD1-N, and pYD1 containing various gene fragments of the N protein. The transformation reactions (100 μ L/

sample) were spread on leucine-containing minimal dextrose plates, which were then incubated at 30 °C for 2–4 days until single colonies appeared.

INDUCTION OF YEAST SURFACE-DISPLAYED FUSION PROTEIN

To express fusion protein on the EBY100 yeast cell surface, transformants were grown in glucose-containing medium overnight, then switched to a medium containing galactose for induction of expression. The experimental procedures described below were applied according to the manufacturer's instructions and a previously published protocol (30). Briefly, a single yeast colony (i.e., untransformed EBY100, EBY100/pYD1, EBY100/pYD1-N, and EBY100/pYD1 containing various N protein fragments) was inoculated into 8 mL of yeast nitrogen-based casamino acid medium containing 20 g/L glucose and grown overnight at 30 °C with shaking. When the A_{600} readings reached 5, the cell cultures were centrifuged at 3000g to 5000g for 5 min at room temperature. The cell pellets were resuspended in yeast nitrogen-based casamino acids medium containing 20 g/L galactose to an A_{600} of 0.5–1, ensuring that the cells continued to grow in a log-phase pattern. Yeast cells were incubated at 20 °C with shaking. The cell cultures were assayed over a 48-h period (at 0, 12, 24, 36, and 48 h) to determine the optimum induction time for maximum display. The maximum display of fusion proteins on the EBY100 cell surface was observed 24–36 h after induction. The optimum displayed yeast cultures were stored at 4 °C for analysis.

FLUORESCENT LABELING OF YEAST SURFACE-DISPLAYED PROTEINS

Anti-Xpress-FITC antibody was purchased from Invitrogen and Anti-6 × His antibody from Roche Applied Science. We obtained 14 mAbs against the SARS-CoV N protein. FITC-conjugated goat anti-mouse IgG and FITC-conjugated goat anti-human IgG were purchased from Beijing Zhongshan Golden Bridge Biotechnology Co., Ltd. For the fluorescent labeling of yeast surface-displayed proteins, 1×10^6 yeast cells were microcentrifuged. The cell pellets were resuspended in ice-cold PBS (0.01 mol/L, pH 7.2–7.4) containing 1 g/L bovine serum albumin and washed twice. The cell pellets were resuspended in 100 μ L of PBS containing either the primary antibody against the epitope tags (i.e., Xpress or 6 × His tag) or the SARS-CoV N-protein-specific mAbs and incubated at 4 °C for 30 min. The cells were then added to 100 μ L of PBS containing the fluorescently labeled secondary antibody (FITC-conjugated goat anti-mouse IgG or FITC-conjugated goat anti-human IgG) at titers of 1:50, incubated at 4 °C for 1 h in the dark, and then washed twice with 0.8 mL of ice-cold PBS. Finally, the yeast cells were resuspended in 300 μ L of PBS and kept at 4 °C until flow cytometry analysis. To distinguish the linear from the conformational epitopes of the SARS-CoV N protein, yeast cells were heated to 80 °C for 30 min in a thermostatically controlled water bath and then chilled on ice 20 min before labeling with antibodies (30). The specific antibody-binding assay was performed with a FACSCal-

ibur flow cytometer (Becton Dickinson Inc), and the results were analyzed by CellQuest Macintosh software (Becton Dickinson).

PREADSORPTION OF SERA FROM HUMANS AND MICE

To identify the presence of epitope-specific antibodies against SARS-CoV N protein in sera, induced EBY100/pYD1 yeast cells (i.e., yeast containing the empty pYD1 vector) were pelleted and washed twice with ice-cold PBS. Serum samples were diluted 1:50 in PBS containing 0.5 g/L sodium azide and mixed with 2×10^6 yeast cells per 50 μ L of attenuated serum. This preadsorption mixture was agitated moderately at 4 °C overnight to eliminate nonspecific binding to yeast surface molecules. After pelleting, the supernatant was recovered and diluted with PBS to a final serum dilution of 1:100. Normal control serum was processed by the same procedure.

Results

GENERATION AND CHARACTERIZATION OF SARS-CoV N-PROTEIN-SPECIFIC mAbs

The isotypes of the 14 mAbs are shown in Table 1. The specificities and immunoreactivities of the mAbs to the SARS-CoV N protein were determined by Western blotting, ELISA, and IFA. Three mAbs (A50, B30, and C31) against the SARS-CoV spike protein S1 domain at N-terminal residues 249–667 (31) were used as negative controls (Table 1).

Among the 14 mAbs tested in the ELISA, 5 (M1, M3, M6, M9, and M11) exhibited a strong positive signal, 8 (M2, M4, M5, M7, M8, M10, M13, and M14) an intermediate signal, and 1 (M12) reacted positively with the N protein. mAbs M9 and M11 had strong reactivity with SARS-CoV N protein in Western blotting analysis, mAbs M4 and M6 had moderate reactivity with the N protein, and the remaining mAbs showed weak or no reactivity with the N protein. To determine the cross-reactivity of these 14 mAbs with other human coronavirus strains, Vero E6 cells infected with SARS-CoV, MRC-5 cells infected with CoV 229E, and BS-C-1 cells infected with CoV OC43 were processed by indirect IFA. All 14 mAbs showed a positive signal to Vero E6 cells infected with SARS-CoV but no reactivity with MRC-5 cells infected with CoV 229E or BS-C-1 cells infected with CoV OC43. The IFA results indicate that the SARS-CoV N-protein-specific mAbs generated in this study did not cross-react with other human coronavirus strains.

YEAST CELL SURFACE DISPLAY OF FULL-LENGTH SARS-CoV N PROTEIN AND ITS OVERLAPPING FRAGMENTS

On the basis of the epitope prediction of the SARS-CoV N protein (Fig. 1A), we designed 7 series-truncated and 4 nested-deletion fragments (Fig. 1B). The yeast expression plasmid pYD1 containing the full-length N protein and a panel of fragments encoding various N genes were transformed into the yeast *Saccharomyces cerevisiae* EBY100 strain and then induced for protein expression. The his-

Table 1. Characterization of the 14 SARS-CoV N-protein-specific mAbs.

mAb ^a	Isotype	Reaction with N protein		IFA result from cells infected by ^d		
		ELISA ^b	Western blot ^c	SARS-CoV	CoV 229E	CoV OC43
M1	IgG2a	+++	+W	+	-	-
M2	IgG1	++	+W	+	-	-
M3	IgG1	+++	+W	+	-	-
M4	IgG1	++	+M	+	-	-
M5	IgG1	++	+W	+	-	-
M6	IgG1	+++	+M	+	-	-
M7	IgG2b	++	+W	+	-	-
M8	IgG2b	++	+W	+	-	-
M9	IgG1	+++	+S	+	-	-
M10	IgG2b	++	-	+	-	-
M11	IgG2a	+++	+S	+	-	-
M12	IgG1	+	+W	+	-	-
M13	IgG2b	++	-	+	-	-
M14	IgG1	++	+W	+	-	-
A50	IgG1	-	-	/	/	/
B30	IgG2a	-	-	/	/	/
C31	IgG2a	-	-	/	/	/

^a Fourteen N-protein-specific mAbs were generated and designated M1 to M14; 3 mAbs (A50, B30, and C31) against the SARS-CoV spike protein S1 domain at N-terminal residues 249–667 were used as negative controls in these assays.

^b The purified recombinant N protein (5 mg/L, 100 μ L/well) was used as the coating antigen and was reacted with purified anti-N-protein mAb. The absorbance was measured at 450 nm: -, negative result; +, $A_{450} = 0.2-1$; ++, $A_{450} = 1-2$; +++, $A_{450} > 2$.

^c The purified recombinant N proteins were transferred to polyvinylidene fluoride membranes, blotted with purified mAbs, and visualized with aminooethyl carbazole chromogen: -, no reactivity; +W, weak positive signal; +M, medium positive signal; +S, strong positive signal.

^d The indirect immunofluorescence staining was assessed in Vero cells infected with SARS-CoV, MRC-5 cells infected with human CoV 229E, and BS-C-1 cells infected with human CoV OC43: -, negative result; +, positive signal; /, not tested.

tograms of detected SARS-CoV N protein and its fragments displayed on the EB100 yeast cell surface are presented in Fig. 2. In this yeast display system, a percentage of cells did not express protein on their surface, and as a result 2 histogram peaks occurred. The flow cytometry histograms of the positive yeast display showed a peak with background fluorescence equivalent in intensity to that obtained with negative controls, which also provided a good internal negative control of the labeling (30).

The full-length SARS-CoV N protein (amino acids 1–422) was expressed on the yeast cell surface, as indicated by reactivity of the Xpress epitope tag with the anti-Xpress antibody (Fig. 2). The N protein fragments NT1 (amino acids 1–69), NT2 (amino acids 68–120), NT3 (amino acids 119–213), NT4 (amino acids 212–341), NT5 (amino acids 337–422), NNDC1 (amino acids 68–213), NNDC2 (amino acids 214–422), NND13 (amino acids

1–120), and NND14 (amino acids 1–213) were also well expressed as detected by the Xpress or 6 \times His epitope tags (Fig. 2). The fragment NND15 (amino acids 1–341) was not expressed on the yeast cell surface; its absence suggests that this fragment corresponds to unstable protein-domain breakpoints that could not be properly folded or trafficked through the yeast secretory pathway (32, 33), and it was removed from further functional studies. The well-expressed yeast-displayed fusion proteins and the well-characterized N-protein-specific mAbs were used for antibody epitope mapping.

ANTIBODY EPITOPE MAPPING OF THE SARS-CoV N PROTEIN

The 14 mAbs were used in the same concentration (10 mg/L per sample) and diluted into PBS in a final volume of 100 μ L for the binding assay. All assays were performed in triplicate or more, and the individual fluorescence intensities were obtained from the mean value of the specific yeast-displayed protein. The ratio of the recombinant antigen expression on the yeast surface (RAYS) was calculated by dividing the fluorescence intensity obtained for the individual RAYS by the fluorescence intensity obtained from yeast expressing pYD1 (i.e., EB100/pYD1). A ratio ≥ 2 was considered positive (34). EB100 yeast cells displaying irrelevant antigens, decay-accelerating factor, and isotype-matched control antibodies were used as negative controls for the 14 mAbs and 10 yeast-displayed fusion proteins. The negative controls did not show any specific binding (data not shown). The profile of the antibody epitope mapping of the SARS-CoV N protein is summarized in Table 2.

The antigenic determinant sites located on the N protein were determined according to the specific binding of a mAb to the particular yeast-displayed protein. Flow cytometric analysis showed prominent immunoreactivity to the full N protein (amino acids 1–422) for 7 of the 14 mAbs (M1, M3, M4, M5, M6, M7, and M9), demonstrating that yeast surface-display technology is a useful method for biochemical characterization of ligand-receptor interactions and antibody-binding epitopes. The antigen-antibody response of NND14 (amino acids 1–213) was as strong as, or in some cases stronger than, that of the full-length N protein (amino acids 1–422). In addition to the full N protein (amino acids 1–422) and NND14 (amino acids 1–213), NNDC2 (amino acids 214–422) showed specific binding to mAbs M2, M8, M10, M11, M12, M13, and M14. On the basis of these experimental data, the 14 mAbs were definitively divided into 2 different groups: mAbs M1, M3, M4, M5, M6, M7, and M9, which recognized the full N protein (amino acids 1–422) as well as the N-terminal fragment of NND14 (amino acids 1–213); and mAbs M2, M8, M10, M11, M12, M13, and M14, which reacted only with the C-terminal fragment of NNDC2 (amino acids 214–422).

mAbs M3 and M9 displayed strong immunoreactivity with the full-length N protein (amino acids 1–422),

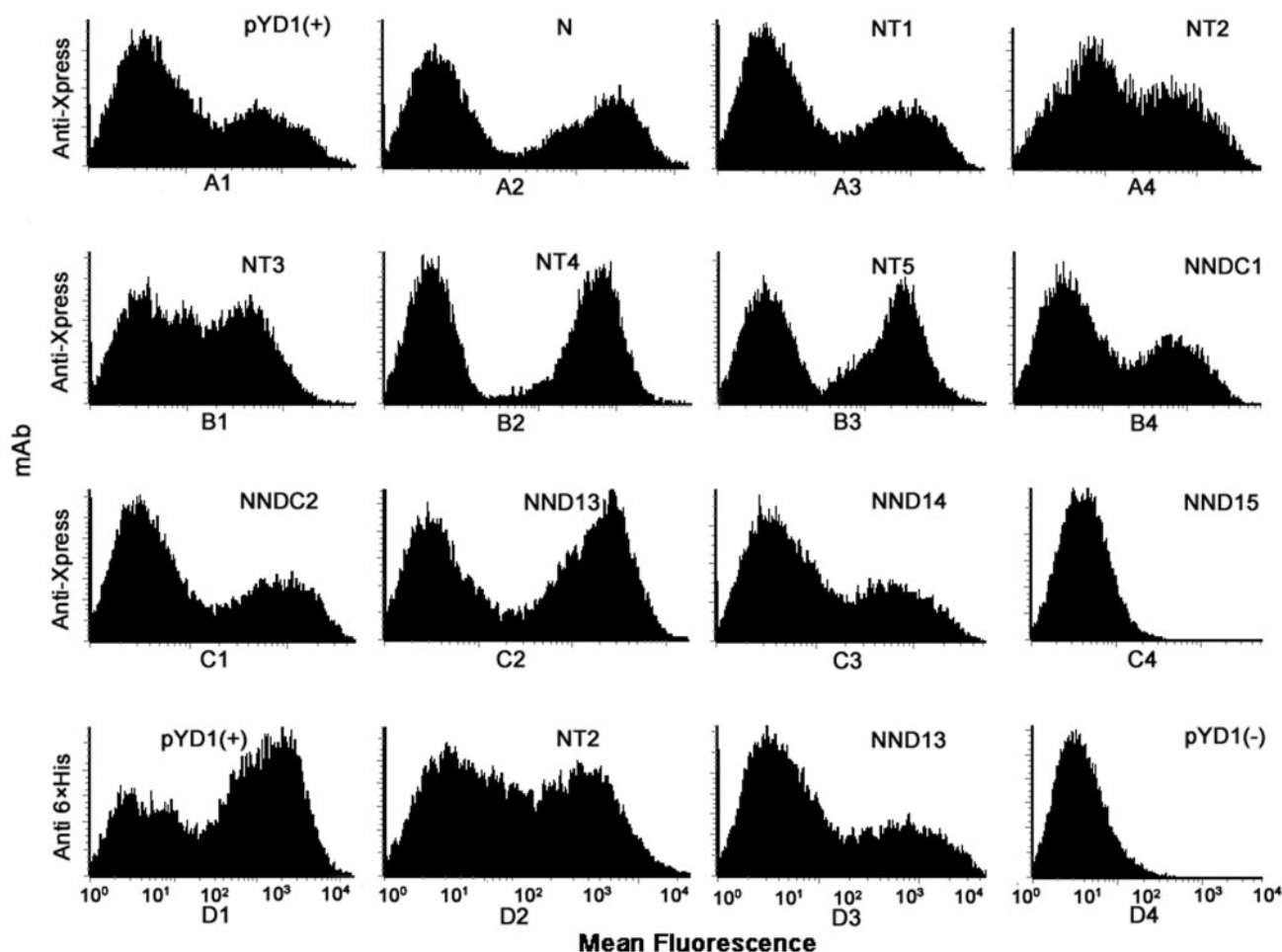


Fig. 2. Detection of the SARS-CoV N protein and its fragments displayed on the EB Y100 yeast cell surface.

Representative flow cytometry histograms depict the mean fluorescence signals for antibody labeling of the N-terminal Xpress and C-terminal 6 × His epitope tags of yeast-displayed fusion proteins. Anti-Xpress labeling of the N-terminal Xpress and anti-6 × His antibody labeling of the C-terminal 6 × His tags expressed on EB Y100/pYD1 were used as positive controls (A1 and D1). EB Y100/pYD1 labeled with only the FITC-conjugated second antibody was used as a negative control (D4). The double peaks show the reactivity of the anti-Xpress antibody with the N-terminal Xpress epitope tag (A2–A4, B1–B4, and C1–C3) and the anti-6 × His antibody with the C-terminal 6 × His tag (D2 and D3) of EB Y100/pYD1 containing the full-length N protein and its fragments. EB Y100/pYD1 containing the fragment NND15 showed no reactivity with the anti-Xpress antibody labeling (C4), indicating that this fragment was not expressed by yeast cells.

NND14 (amino acids 1–213), NND13 (amino acids 1–120), and NT1 (amino acids 1–69), but not with NT2 (amino acids 68–120) or NT3 (amino acids 119–213). The mAb M3- and M9-specific epitopes thus are located in the region of amino acids 1–69. The binding of mAb M13 to both NNDC2 (amino acids 214–422) and NT4 (amino acids 212–341) and exclusively to NT4 (amino acids 212–341) suggests that the mAb M13-specific epitope is situated between residues 212 and 341. mAbs M10 and M11 reacted with NNDC2 (amino acids 214–422) and NT5 (amino acids 337–422). The mAb M10- and M11-specific epitopes are therefore located in the region including amino acids 337–422 on the N protein.

Because mAbs M1, M4, M5, M6, and M7 bound to the full N protein (amino acids 1–422), NND14 (amino acids 1–213), and NNDC1 (amino acids 68–213) but not with NT1 (amino acids 1–69), NT2 (amino acids 68–120), or

NND13 (amino acids 1–120), we deduced that the antigenic sites corresponding to these 5 antibodies were in the region of amino acids 68–213 on the N protein. Three (M1, M6, and M7) of these 5 mAbs exhibited slight binding to NT3 (amino acids 119–213), further confirming the antigenicity of the region of amino acids 68–213. We speculated that the major portion involved in the antibody-binding sites of mAbs M2, M8, M12, and M14 is localized in the central region of Ala337 to Asp341 of the breakpoint of NT4 (amino acids 212–341) and NT5 (amino acids 337–422) in the region of fragment NNDC2 (amino acids 214–422) on the N protein.

Fragment NT2 (amino acids 68–120) did not bind to any of the 14 mAbs, indicating that the antibody-binding epitope may flank the breakpoint of the particular fusion protein tested or that we did not produce a mAb specific to the antigenic site within NT2 (amino acids 68–120).

Table 2. Antibody epitope mapping of SARS-CoV N protein with mAbs.^a

mAb ^b	Flow cytometry results ^c									
	Full-length N (1–422)	NND14 (1–213)	NND13 (1–120)	NNDC1 (68–213)	NT1 (1–69)	NT2 (68–120)	NT3 (119–213)	NNDC2 (214–422)	NT4 (212–341)	NT5 (337–422)
M1	++	+++	–	++	–	–	+	–	–	–
M2	–	–	–	–	–	–	–	++	–	–
M3	+++	+++	+++	–	+++	–	–	–	–	–
M4	++	+++	–	++	–	–	–	–	–	–
M5	++	+++	–	++	–	–	–	–	–	–
M6	++	+++	–	++	–	–	+	–	–	–
M7	++	+++	–	++	–	–	+	–	–	–
M8	–	–	–	–	–	–	–	++	–	–
M9	+++	+++	+++	–	+++	–	–	–	–	–
M10	–	–	–	–	–	–	–	+++	–	+++
M11	–	–	–	–	–	–	–	+++	–	+++
M12	–	–	–	–	–	–	–	++	–	–
M13	–	–	–	–	–	–	–	+++	+++	–
M14	–	–	–	–	–	–	–	+++	–	–

^a Ten variable fragments distributed on the N protein were displayed on the EBY100 yeast cell surface to measure binding with the mAbs. The numbers in parentheses represent the amino acid numbers of the start and stop positions on the N protein.

^b The 14 mAbs produced in this study were used in this assay.

^c The fluorescence intensities of the various yeast-displayed fusion proteins binding to the 14 mAbs determined by flow cytometry were calculated by dividing the fluorescence intensity obtained for the individual fusion proteins by the fluorescence intensity obtained for the yeast expressing empty vector pYD1. Values with a ratio ≥ 2 were considered positive: –, negative result (ratio < 2); +, weak but detectable positive signal (ratio 2–5); ++, intermediate positive signal (ratio 5–10); + + +, strong positive signal (ratio > 10).

LINEAR VS CONFORMATIONAL SARS-CoV N PROTEIN-SPECIFIC mAb EPITOPES

We used heat denaturation of the fusion proteins tethered to the EBY100 yeast cell surface to categorize the specific linear and conformational SARS-CoV N protein mAb epitopes (35,36). Anti-Xpress and anti-6 × His label mAbs were set as positive controls to identify the Xpress and 6 × His epitope tags flanking the fragment inserts before and after the yeast-displayed fusion protein denaturation and to verify that the protein and yeast cells were not compromised during the heat treatment. To further confirm the denaturation of yeast-displayed proteins on heat treatment and as a positive control, we simultaneously assayed the yeast cells binding to the specific mAbs obtained. We calculated the RAYS ratio by dividing the fluorescence intensity obtained for the individual RAYS by the fluorescence intensity obtained for yeast expressing pYD1 before and after heat denaturation. A ratio ≥ 2 was considered positive. The flow cytometry results are expressed as RAYS ratios to assess the antigen-antibody binding and the RAYS ratios representing specific binding of yeast-displayed proteins to mAbs before and after heat denaturation. The RAYS ratios before and after denaturation and the overall distinction between linear and conformational antigenic determinants of the SARS-CoV N protein are shown in Fig. 3.

The binding of NT1 to mAb M3 was abolished by heat treatment, indicating that mAb M3 reacted with continuous or discontinuous conformational determinants. This explanation is supported by the abolition of the binding of the full-length N protein and fragments NND14 and

NND13 to mAb M3 after heat denaturation (Fig. 3, A and B). The mAb M3-specific conformational epitope was identified and localized in the region of amino acids 1–69 on the N protein. The reactivities of mAb M13 to NT4 and mAb M10 to NT5 disappeared after denaturation, suggesting that M13- and M10-specific antibody epitopes located on the N protein fragments NT4 and NT5, respectively, are conformational determinants (Fig. 3C). Except for the conformational epitopes identified above, mAbs M1, M4, M5, M6, and M7 reacted with conformational epitopes located between amino acids 68 and 213 (Fig. 3D). Heat denaturation abolished the specific binding (Fig. 3C) of mAbs M2, M8, M12, and M14, which had been raised against fragment NNDC2 before heat treatment, showing that these reacted with discontinuous epitopes.

mAb M9 retained its immunoreactivity with the N protein and with NT1, NND13, and NND14 after heat treatment and showed binding to linear or sequential epitopes other than those bound by mAb M3 (Fig. 3, A and B). Similarly, the binding of mAb M11 to NNDC2 and NT5 was maintained after heat treatment, indicating that the mAb M11 antibody-binding epitope is linear and different from that of mAb M10 (Fig. 3C). The 2 identified linear epitopes localized in the regions of amino acids 1–69 and 337–422 on the N protein are consistent with previously published data from studies using the synthesis of overlapping or mutated peptides (21, 22, 24) and prokaryotic expression of SARS-CoV N protein segments (25) to probe sera from convalescent SARS patients. Although these studies found that heterogeneous specific

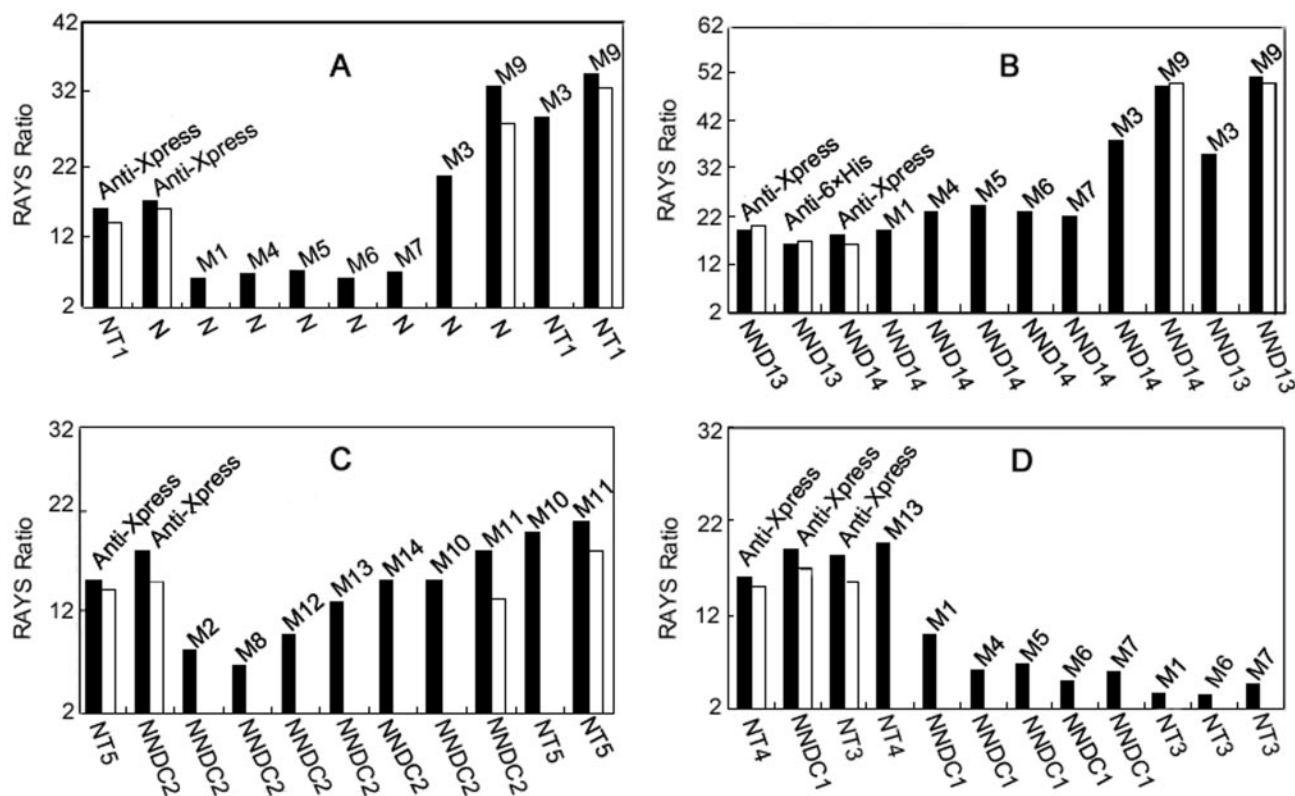


Fig. 3. Linear vs conformational SARS-CoV N-protein-specific mAb epitopes classified by mAb labeling of the yeast-displayed fusion protein before (■) and after (□) heat denaturation.

The fluorescence intensity was calculated as a RAYS ratio. A RAYS ratio of 2 was set as the baseline, and a RAYS ratio >2 was considered positive. The Xpress and $6 \times$ His epitope tags flanking the gene inserts on the yeast-displayed fusion proteins were determined to validate that the protein and yeast cell were not damaged during the heat treatment. mAbs with known binding to specific yeast-displayed proteins before denaturation were labeled simultaneously as a parallel control. Shown are representative interactions between yeast-displayed fusion proteins and the specific mAbs tested.

synthetic peptides reacted with the sera from SARS patients, the most immunoreactive oligopeptides were located mainly within the 2 separate regions (amino acids 1–69 and 337–422) of the N protein, as described above.

IMMUNODOMINANT EPITOPES LOCATED ON THE N PROTEIN SCREENED BY ANTISERA FROM IMMUNIZED MICE

To distinguish the immunodominant linear from the conformational antigenic structures of the SARS-CoV N protein, 4 mice were immunized with the N protein and the antisera were collected. Strong anti-N-protein antibody responses were detected by ELISA in sera from the 4 immunized mice but not in sera from 2 nonimmunized control mice (data not shown). This result demonstrates that N protein is one of the immunoreactive coronavirus structural proteins that elicit the specific humoral immune responses in animals.

EBY100-pYD1 yeast cells were used to preadsorb mouse antisera to eliminate the nonspecific binding to yeast surface molecules in the reactions, as described above. The reactivity of the full-length N protein and its overlapping fragments before and after denaturation with the mouse antisera was detected by flow cytometry. No positive signals were detected in reactions containing

control sera from 2 nonimmunized BALB/C mice and the fusion proteins (data not shown).

As shown in Fig. 4, yeast-displayed SARS-CoV N protein reacted with the antisera from the 4 mice. The immunoreactivity of the protein fragments with polyclonal antisera from immunized mice confirmed the identification of the antigenic sites on the N protein by mAbs, as described above (Fig. 3). Fragments NT1, NT3, NT5, NND13, NND14, NNDC1, and NNDC2 reacted with antisera both before and after denaturation (Fig. 4), indicating that both immunodominant linear and conformational epitopes are located in the regions containing amino acids 1–69, 70–213, and 337–422. After denaturation, fragment NT4 gave positive signals in the antisera from 2 mice (Fig. 4, antisera from mice 1 and 4), and fragment NT2 was positive in the antisera from 3 mice (Fig. 4, antisera from mice 1, 2, and 3), suggesting that these regions also bear the linear epitopes. The reactivity of the N protein fragments with mouse antisera indicated that the regions containing amino acids 1–69, 121–213, and 337–422 are the dominant antigenic regions within the full-length N protein. The antigenic domains on the N protein (Fig. 1D) have potential as diagnostic markers and

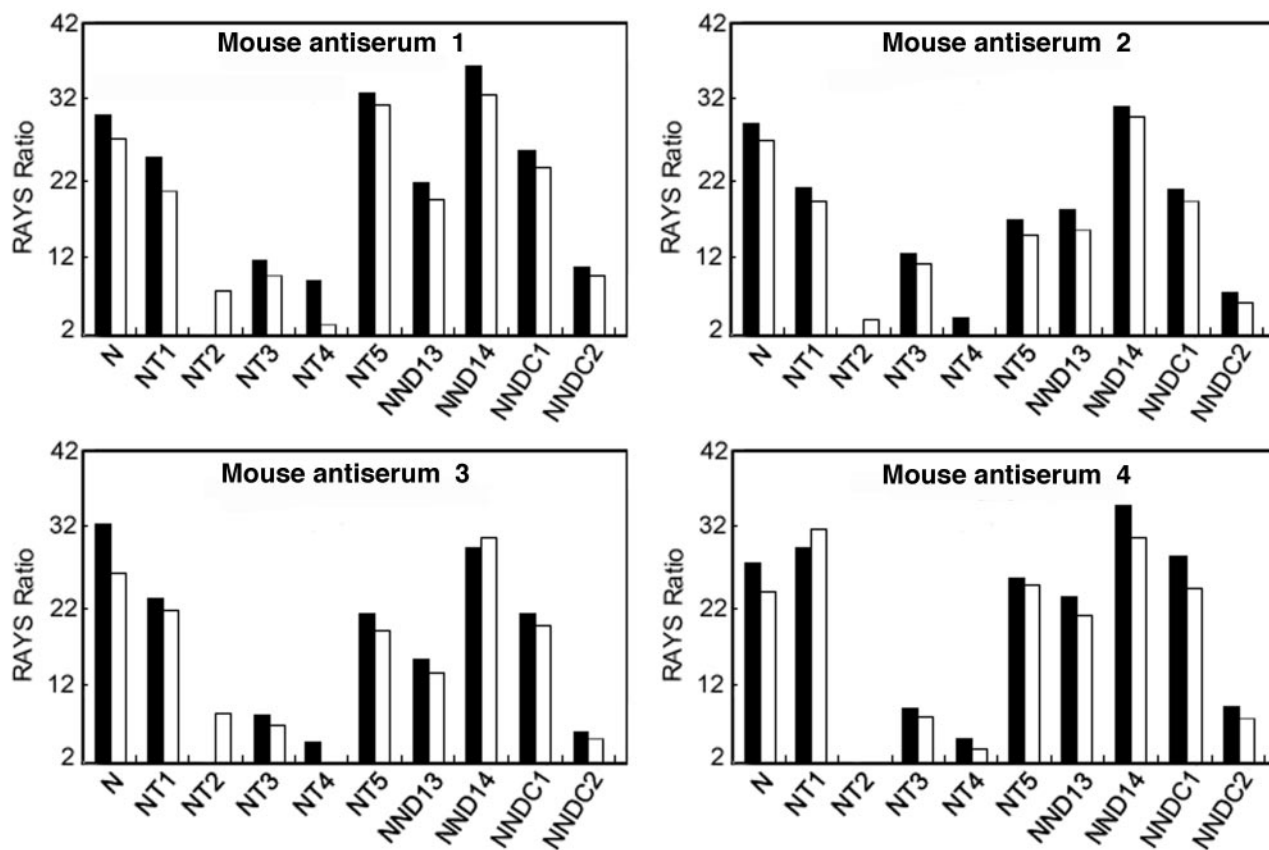


Fig. 4. Flow cytometric analysis of the immunodominant epitopes on the N protein in the antisera from 4 mice.

The reactivities with the mouse antisera were determined in the yeast-displayed fusion proteins before (■) and after (□) denaturation. The flow cytometry data are expressed as RAYS ratios to illustrate the immunoreactivities of the different regions of the N protein.

may represent potential antiviral targets for vaccine development.

VERIFICATION OF IDENTIFIED IMMUNODOMINANT EPITOPES ON THE N PROTEIN WITH SERA FROM SARS PATIENTS

We next validated the antigenicity of the identified immunodominant epitopes to gain insight into the humoral immune response to the SARS-CoV N protein in humans. Forty serum samples from patients with atypical pneumonia identified by our assay were numbered from 1 to 40, and the sera of cases 21–40 were pooled for flow cytometric analysis. Sera collected from 40 healthy blood donors and sera from 38 patients with upper respiratory symptoms who were not infected with the SARS virus during the atypical pneumonia pandemic in 2003 were simultaneously assayed as individual or pooled samples to provide negative controls. All assays were performed in triplicate or more. No positive signals were detected in the yeast-displayed fusion proteins that reacted with the control sera in both individual and pooled samples (data not shown). The data for the 10 yeast-displayed fusion proteins before and after denaturation in cases 1–20 and in the pooled sera from SARS patients are shown in Table 3 and Fig. 5.

Both before and after denaturation, the EBY100-dis-

played N protein reacted with the antibodies raised in the sera from SARS patients, as indicated by RAYS ratios >2. Twenty-one serum preparations (sera of cases 1–20 and the serum pooled from cases 21–40) were immunopositive, demonstrating that the N protein is an immunodominant antigen in SARS-CoV-infected patients with atypical pneumonia. In addition to the full-length N protein, both before and after heat treatment, fragments NT1, NT5, NND13, NND14, and NNDC1 reacted with the pooled sera. NT3 also reacted with the serum pool from SARS patients after denaturation (Table 3 and Fig. 5F). Fragment NND14 reacted with sera from 19 of 20 cases before denaturation and all 20 cases after denaturation, a reactivity similar to that obtained by probing with the full-length N protein. The reactivity of yeast-displayed proteins with various N protein fragments probed with the sera from SARS patients suggests that 6 or more immunodominant epitopes are located on the N protein (Fig. 5).

Fragment NT1 reacted with the sera from 17 of 20 cases before denaturation and 16 of 20 cases after denaturation. Fragment NND13 reacted with the sera from 10 of 20 cases before denaturation and 8 of 20 after denaturation. Fragment NT2 did not react with any of the sera tested. These data indicate that NT1 contains both the immunodominant linear and conformational epitopes. These data

Table 3. Serologic analysis of the anti-N-protein immune response obtained by reaction of the yeast-displayed fusion proteins with sera from convalescent SARS patients.

Sera ^a	Reactivity based on RAYS ratio ^b									
	Full-length N ^c (1-422)	NT1 (1-69)	NT2 (68-120)	NT3 (119-213)	NT4 (212-341)	NT5 (337-422)	NND13 (1-120)	NND14 (1-213)	NNDC1 (68-213)	NNDC2 (214-422)
Case 1	+/+	+/+	-/-	-/+	-/-	+/+	+/-	+/+	+/+	-/-
Case 2	+/+	+/+	-/-	-/-	-/-	-/+	+/+	+/+	+/-	-/-
Case 3	+/+	+/-	-/-	-/+	-/-	+/+	-/-	+/+	+/+	+/-
Case 4	+/+	+/+	-/-	-/-	+/-	+/+	+/-	+/+	+/+	-/+
Case 5	+/+	-/+	-/-	-/+	-/-	+/-	-/+	+/+	-/-	-/+
Case 6	+/+	+/+	-/-	+/+	-/-	+/+	-/-	+/+	+/+	-/-
Case 7	+/+	+/+	-/-	-/-	-/-	+/+	+/+	+/+	+/-	-/-
Case 8	+/+	+/+	-/-	+/+	+/-	-/+	-/-	+/+	+/+	-/-
Case 9	+/+	-/+	-/-	-/-	-/-	+/+	+/-	+/+	+/+	-/+
Case 10	+/+	+/+	-/-	-/+	-/-	+/+	-/+	+/+	+/+	-/-
Case 11	+/+	+/+	-/-	+/+	-/-	-/+	+/+	+/+	+/+	-/-
Case 12	+/+	+/+	-/-	-/-	-/-	+/+	-/-	+/+	+/+	-/-
Case 13	+/+	+/+	-/-	-/+	-/-	+/+	-/+	+/+	+/+	+/-
Case 14	+/+	+/-	-/-	-/-	-/-	+/+	+/-	-/+	+/-	-/-
Case 15	+/+	-/+	-/-	-/+	+/-	+/+	-/+	+/+	+/+	-/-
Case 16	+/+	+/+	-/-	-/+	-/-	+/+	+/-	+/+	+/+	-/-
Case 17	+/+	+/-	-/-	-/+	-/-	+/-	-/-	+/+	+/+	-/-
Case 18	+/+	+/+	-/-	-/+	-/-	+/+	+/+	+/+	+/-	-/-
Case 19	+/+	+/-	-/-	-/+	-/-	+/+	+/-	+/+	+/+	-/-
Case 20	+/+	+/+	-/-	-/-	-/-	+/+	-/-	+/+	+/+	-/-
Pooled ^d	+/+	+/+	-/-	-/+	-/-	+/+	+/+	+/+	+/+	-/-

^a The sera from individual convalescent SARS patients were numbered case 1 to 20.

^b RAYS ratios before/after denaturation of the particular displayed fusion protein: +, RAYS ratio ≥ 2 (positive); -, RAYS ratio < 2 (negative). The RAYS ratio was calculated as described in the text.

^c Ten proteins, including the full-length N protein and its fragments displayed on the yeast EBY100 cell surface before and after denaturation, were used in this assay. The numbers in parentheses represent the amino acid numbers of the start and stop positions on the N protein.

^d Pooled sera was obtained by mixing the sera from SARS cases 21-40.

are consistent with the antisera analyses and with the mAb epitope-mapping analysis showing that mAb M3- and M9-specific epitopes are located between amino acids 1 and 69 of the N protein (Fig. 4).

Fragment NNDC1 reacted with pooled sera and with sera from 19 of 20 cases before denaturation and with 15 of 20 after denaturation. NT3 reacted with the sera of 3 of 20 cases before denaturation and 13 of 20 after denaturation. Fragment NT2 did not produce a positive signal with any of the sera from SARS patients. After comparing the analytical results of epitope mapping in the antisera and the current data, we deduced that the conformational epitopes are located between amino acids 68 and 213 on the N protein and that the epitope responsible for antibodies in the sera of SARS patients lies in the region of amino acids 121-213 of denatured NNDC1. Because none of the 14 mAbs reacted with the denatured fragments NNDC1 or NT3, we did not obtain hybridoma antibodies raised against the linear epitope located in the region containing amino acids 121-213.

Fragment NT5 reacted with mAb M10 before denaturation, with mAb M11 before and after denaturation, and with antisera from the 4 immunized mice. This fragment was immunopositive with the pooled sera and the sera

from 17 of 20 cases before denaturation and with the sera from 18 of 20 of cases after denaturation. In contrast, NNDC2 was immunopositive with sera from only 2 of 20 cases before denaturation and 3 of 20 cases after denaturation and was not positive with the pooled sera. These data suggest that NT5 contains both linear and conformational immunodominant epitopes.

Fragment NT4 reacted with the sera from only 3 of 20 cases before denaturation, indicating that the mAb M13-specific conformational epitope located within NT4 (amino acids 212-341) is the minor immunodominant epitope.

We detected 3 conformational immunodominant epitopes located in the regions containing amino acids 1-69, 68-213, and 337-422 on the N protein and 3 linear immunodominant epitopes in the regions containing amino acids 1-69, 121-213, and 337-422 in the sera from SARS patients (Fig. 1C). The immunodominant antigenic structures identified by the antibodies raised in the sera from SARS patients are consistent with those obtained from the mAbs and mouse antisera. These data demonstrate that the SARS-CoV N protein is one of the immunodominant viral proteins and that 3 domains (amino

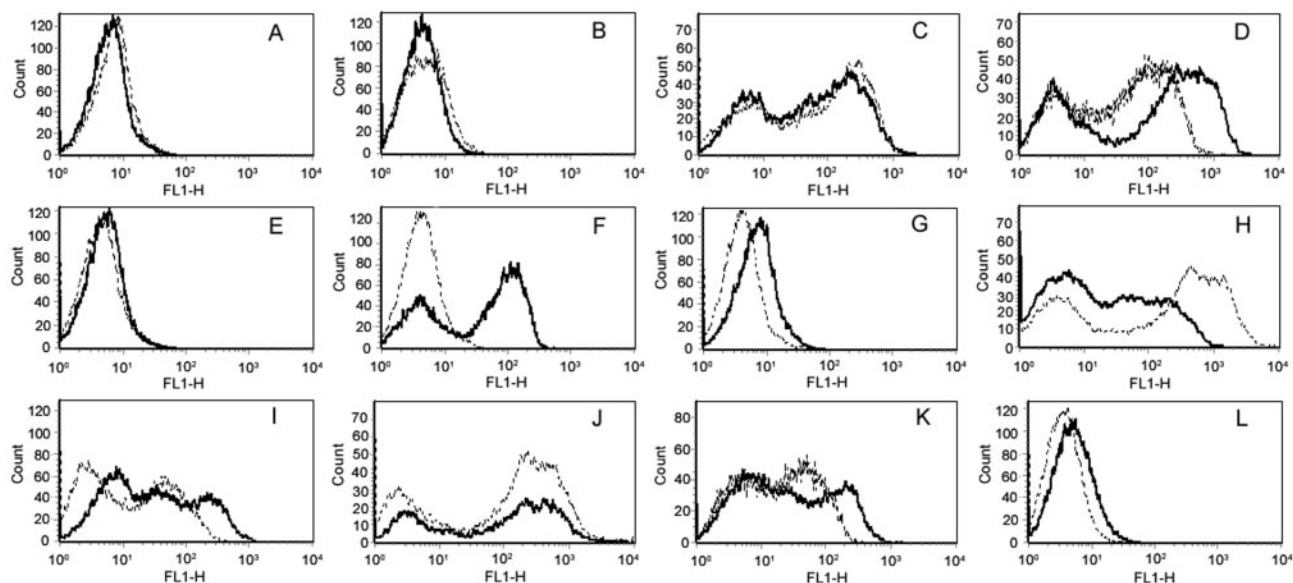


Fig. 5. Reactivity of the yeast-displayed fusion proteins with the antibodies raised in the sera of SARS patients.

The flow cytometry histograms represent the mean fluorescence intensities of the specific yeast-displayed fusion proteins before (dotted line) and after (solid line) denaturation. The yeast pYD1 cells that reacted with the pooled normal sera from healthy volunteers (A) and pooled sera from patients with upper respiratory symptoms but not infected with SARS (B) were included as negative controls. The full-length protein N (C) and fragments NT1 (D), NT3 (F, after denaturation), NT5 (H), NND13 (I), NND14 (J), and NND1 (K) were immunopositive with the pooled sera of the SARS patients. The antibodies in the pooled sera from SARS patients were not detected by probing with NT2 (E), NT3 (F, before denaturation), NT4 (G), or NND2 (L). Because the reactivities of the displayed N protein and its fragments with pooled control sera were negative, the flow cytometry histograms are not included.

acids 1–69, 121–213, and 337–422) are responsible for the immunoreactivity (Fig. 1D).

Discussion

We identified 5 conformational (amino acids 1–69, 68–213, 212–341, 337–422, and 214–422) and 3 linear (amino acids 1–69, 121–213, and 337–422) epitopes on the full-length N protein (Fig. 1C). Our subsequent determination of the antigenic structures of the N protein responsible for antibodies in polyclonal antisera from immunized mice and sera from convalescent SARS patients demonstrated the immunogenic specificity of 3 conformational (amino acids 1–69, 68–213, and 337–422) and 3 linear (amino acids 1–69, 121–213, and 337–422) epitopes (Fig. 1C). We also found 4 novel conformational antigenic sites (amino acids 1–69, 68–213, 212–341, and 337–422; Fig. 1C). The antibody responses of the N protein fragments with mammalian sera revealed that 3 regions of the N protein are strong antigenic domains (Fig. 1D).

Diverse antigenic sites on the SARS-CoV N protein have been identified in the sera of SARS patients and in mouse antiserum (21–25). Although the amino acid sequence of the immunodominant epitope may be involved in these peptides and in protein segments expressed by prokaryotes, it is unlikely that polyclonal serum is sufficient to distinguish the linear from the conformational antigenic structures of individual antigenic domains and the minor or nonimmunodominant epitopes of the N protein (26). The linear epitopes of the N protein identified by probing the sera from SARS patients with synthetic peptides or protein segments expressed by pro-

karyotes (21–23, 25) were limited to the strongly immunodominant antigenic sites. For example, the linear epitope located in the region of amino acids 1–69 was not obtained by Pepscan or microarray analysis of sera from SARS patients (21–23). mAbs provide a more powerful tool than polyclonal serum or animal antiserum for defining the antigenic structures of a given protein in the context of the antigen–antibody interactions and play a vital role in studies of viral antigenicity and immunology (27). Using a combined approach involving the N-protein-specific mAbs, mouse antisera, and sera from SARS patients, we demonstrated that the mAb M9- and M11-specific linear epitopes were located in the regions containing amino acids 1–69 and 337–422 of the N protein, respectively. Using polyclonal sera, we also observed that the third immunodominant linear epitope was located in the region containing amino acids 121–213 on the N protein. The linear epitopes on the N protein that we identified are consistent with those reported previously, although we were able to obtain a better specificity.

We believe that it was necessary to use a eukaryotic system, such as the yeast surface display, to characterize the conformational epitopes of the N protein and specifically to differentiate antibodies raised to the linear from those raised to the conformational immunodominant epitopes in mammalian sera. The yeast surface display is a useful platform in directed evolution of protein expression (30) for the biochemical characterization of antibody-binding sites (35, 36) and for serologic analysis of antigens by recombinant expression cloning (SEREX) (34, 37). The yeast-displayed fusion protein stimulates expression of

the native structure of the protein of interest. Linear epitopes can be distinguished from conformational epitopes on a given protein by analysis of the antigen-antibody interaction before and after heat denaturation of a particular yeast-displayed protein. These features make the yeast display a suitable tool to accurately map the antibody epitope in mAbs, patient serum, and polyclonal antiserum from immunized small animals. For example, using protein microarrays to probe sera from SARS patients, Chen et al. (25) identified conformational epitopes in the regions covering amino acids 51–208 and 249–422 of the N protein. We applied the yeast surface display (34–36) in mAbs and mammalian sera to further define the precise locations of the conformational epitopes within the entire N protein. We first identified mAb M3-, M13-, and M10-specific conformational epitopes located in the regions covering amino acids 1–69, 212–341, and 337–422, respectively (Fig. 1C), and at least 2 other epitopes in the regions covering amino acids 68–213 and 214–422 (Fig. 1C). Three of 5 (amino acids 1–69, 68–213, and 337–422) conformational epitopes were immunodominant, as shown in the sera from SARS patients and the mouse antisera (Fig. 1C). We have expanded the SARS-CoV N protein epitope profile with better specificity than that of previously identified epitopes and have also identified 4 novel conformational epitopes located in the regions covering amino acids 1–69, 68–213, 212–341, and 337–422.

Numerous epidemiologic and serologic studies of SARS-CoV (9–11, 13) have suggested that the SARS-CoV N protein could serve as a diagnostic marker because of its early appearance (11), the long persistence of serum-specific IgG (14), and concordance in sensitive and specific immunoassays (9–11, 14) during SARS infection. The false-positive (38–40) and false-negative (14) results reported by investigators using the recombinant SARS-CoV N-protein-based ELISA and Western blot analysis have raised concerns about using the recombinant full-length N protein, whole-virus antigen extracts, or virus-infected cells as reagents to diagnose SARS-CoV infections in humans and other animal species. Thus, the definite antigenic sites located on the N protein and epitope-specific mAbs identified in our study should enhance accurate serodiagnosis, serosurveillance, and retrospective studies of SARS.

Recent reports of sporadic cases of SARS and the uncertainty of SARS recurrence have prompted the current interest in the pursuit of a SARS-CoV vaccine (41–45). A clear-cut analysis of the humoral immunity induced by active (43–45) and passive (41, 42) immunization with the N protein in the formulation would be a prerequisite for the future use of these vaccines in immunoprophylaxis. Preservation of the conformational antibody-directed epitopes by maintenance of conformational integrity is important in designing recombinant protein vaccines and may require expression in eukaryotic cells (46), which is often neglected in the

development of subunit vaccines. Our data on the N protein epitopes should help uncover the gene products and mechanisms of protective immunity relevant to SARS-CoV. The experimental strategies we describe may facilitate the discovery of epitopes of other structural proteins of SARS-CoV, as well as other viral proteins in humans and other animal species, which may be useful in developing subunit vaccine candidates for antiviral therapy.

The functions of the N protein, such as possible interaction with viral RNA and the composition of the viral core and nucleocapsid (47–49), are well documented in other coronaviruses, and several domains of the N protein play functional roles in viral biology. Primary genomic structural analysis has revealed that the SARS-CoV N protein contains a highly conserved motif located in the region of amino acids 111–118 (FYLLGTGP) (50) and a unique lysine-rich region around amino acids 362–381 (KTFPPTEPKKDKKKKTDEAQ) (51), findings suggesting that the protein acts as a nuclear localization signal (Fig. 1D). The mAb-specific epitopes located in the regions covering amino acids 68–213 and 337–422 on the N protein suggest that mAbs M1, M4, M5, M6, M7, M10, and M11 could serve as biochemical markers to analyze the functional roles of these regions in SARS-CoV pathogenesis in other experimental systems. Although the N-terminal (amino acids 45–181) structure of the SARS-CoV N protein has been determined by nuclear magnetic resonance imaging (52) and this region has been promoted as the putative RNA-binding domain (53), the structure of the full-length N protein has not yet been determined. We found that 7 of 14 mAbs (M1, M3, M4, M5, M6, M7, and M9) reacted only with the yeast-displayed full-length N protein (amino acids 1–422) and the N-terminal fragment (amino acids 1–213), but not with the C-terminal fragment (amino acids 214–422), which specifically reacted with the other mAbs (M2, M8, M10, M11, M12, M13, and M14). This unexpected finding led us to speculate that the C-terminal fragment (amino acids 214–422) is buried within the entire N protein and provides a clue to further explore the native structure of the N protein. The identification of specific antibody-binding sites in our study may assist in determination of the 3-dimensional structure of the full-length N protein and interpretation of the putative role of the N protein in the life cycle of the SARS virus.

Focusing on the epitope information, using N protein-specific mAbs we thoroughly mapped the antigenic determinants distributed on the SARS-CoV N protein. We identified the immunodominant antigenic sites responsible for antibodies in sera from SARS patients and antisera from small animals and used yeast surface display to identify the antigenic structures involved in these natural epitopes. The precise positions of these antigenic structures in the SARS-CoV N protein should be studied further to identify the exact amino acids involved. These antigenic sites of the N protein responsible for humoral

immunity and histopathology will undoubtedly provide significant insight into the pathogenesis of the SARS-CoV and will help in the design of potential molecular targets for new antiviral agents.

This work was supported by grants from the National Key Basic Research Program of China (Grants 2001CB510001 and 2003CB514108), the Key Research Program of the National Natural Science Foundation of China (Grant 30490240), and the National Outstanding Young Scientist Foundation of China (Grant 30325020).

References

- Peiris JS, Lai ST, Poon LL, Guan Y, Yam LY, Lim W, et al. Coronavirus as a possible cause of severe acute respiratory syndrome. *Lancet* 2003;361:1319–25.
- Peiris JS, Yuen KY, Osterhaus AD, Stohr K. The severe acute respiratory syndrome. *N Engl J Med* 2003;349:2431–41.
- Guan Y, Zheng BJ, He YQ, Liu XL, Zhuang ZX, Cheung CL, et al. Isolation and characterization of viruses related to the SARS coronavirus from animals in southern China. *Science* 2003;302:276–8.
- Martina BE, Haagmans BL, Kuiken T, Fouchier RA, Rimmelzwaan GF, Van Amerongen G, et al. Virology: SARS virus infection of cats and ferrets. *Nature* 2003;425:915.
- Cui W, Fan Y, Wu W, Zhang F, Wang JY, Ni AP. Expression of lymphocytes and lymphocyte subsets in patients with severe acute respiratory syndrome. *Clin Infect Dis* 2003;37:857–9.
- Wong RS, Wu A, To KF, Lee N, Lam CW, Wong CK, et al. Haematological manifestations in patients with severe acute respiratory syndrome: retrospective analysis. *BMJ* 2003;326:1358–62.
- Li G, Chen X, Xu A. Profile of specific antibodies to the SARS-associated coronavirus. *N Engl J Med* 2003;349:508–9.
- Peiris JS, Chu CM, Cheng VC, Chan KS, Hung IF, Poon LL, et al. Clinical progression and viral load in a community outbreak of coronavirus-associated SARS pneumonia: a prospective study. *Lancet* 2003;361:1767–72.
- Shi Y, Yi Y, Li P, Kuang T, Li L, Dong M, et al. Diagnosis of severe acute respiratory syndrome (SARS) by detection of SARS coronavirus nucleocapsid antibodies in an antigen-capturing enzyme-linked immunosorbent assay. *J Clin Microbiol* 2003;41:5781–2.
- Woo PC, Lau SK, Tsoi HW, Chan KH, Wong BH, Che XY, et al. Relative rates of non-pneumonic SARS coronavirus infection and SARS coronavirus pneumonia. *Lancet* 2004;363:841–5.
- Woo PC, Lau SK, Wong BH, Chan KH, Chu CM, Tsoi HW, et al. Longitudinal profile of immunoglobulin G (IgG), IgM, and IgA antibodies against the severe acute respiratory syndrome (SARS) coronavirus nucleocapsid protein in patients with pneumonia due to the SARS coronavirus. *Clin Diagn Lab Immunol* 2004;11:665–8.
- Lau SK, Woo PC, Wong BH, Tsoi HW, Woo GK, Poon RW, et al. Detection of severe acute respiratory syndrome (SARS) coronavirus nucleocapsid protein in SARS patients by enzyme-linked immunosorbent assay. *J Clin Microbiol* 2004;42:2884–9.
- Tan YJ, Goh PY, Fielding BC, Shen S, Chou CF, Fu JL, et al. Profiles of antibody responses against severe acute respiratory syndrome coronavirus recombinant proteins and their potential use as diagnostic markers. *Clin Diagn Lab Immunol* 2004;11:362–71.
- Wu HS, Hsieh YC, Su IJ, Lin TH, Chiu SC, Hsu YF, et al. Early detection of antibodies against various structural proteins of the SARS-associated coronavirus in SARS patients. *J Biomed Sci* 2004;11:117–26.
- Daginakatte GC, Chard-Bergstrom C, Andrews GA, Kapil S. Production, characterization, and uses of monoclonal antibodies against recombinant nucleoprotein of elk coronavirus. *Clin Diagn Lab Immunol* 1999;6:341–4.
- Nakanaga K, Yamanouchi K, Fujiwara K. Protective effect of monoclonal antibodies on lethal mouse hepatitis virus infection in mice. *J Virol* 1986;59:168–71.
- Lecomte J, Cainelli-Gebara V, Mercier G, Mansour S, Talbot PJ, Lussier G, et al. Protection from mouse hepatitis virus type 3-induced acute disease by an anti-nucleoprotein monoclonal antibody [Brief Report]. *Arch Virol* 1987;97:123–30.
- Boots AM, Benaissa-Trouw BJ, Hesselink W, Rijke E, Schrier C, Hensen EJ. Induction of anti-viral immune responses by immunization with recombinant-DNA encoded avian coronavirus nucleocapsid protein. *Vaccine* 1992;10:119–24.
- Yu L, Liu W, Schnitzlein WM, Tripathy DN, Kwang J. Study of protection by recombinant fowl poxvirus expressing C-terminal nucleocapsid protein of infectious bronchitis virus against challenge. *Avian Dis* 2001;45:340–8.
- Cavanagh D. Severe acute respiratory syndrome vaccine development: experiences of vaccination against avian infectious bronchitis coronavirus. *Avian Pathol* 2003;32:567–82.
- Guo JP, Petric M, Campbell W, McGeer PL. SARS corona virus peptides recognized by antibodies in the sera of convalescent cases. *Virology* 2004;324:251–6.
- Wang J, Wen J, Li J, Yin J, Zhu Q, Wang H, et al. Assessment of immunoreactive synthetic peptides from the structural proteins of severe acute respiratory syndrome coronavirus. *Clin Chem* 2003;49:1989–96.
- He Y, Zhou Y, Wu H, Kou Z, Liu S, Jiang S. Mapping of antigenic sites on the nucleocapsid protein of the severe acute respiratory syndrome coronavirus. *J Clin Microbiol* 2004;42:5309–14.
- Lin Y, Shen X, Yang RF, Li YX, Ji YY, He YY, et al. Identification of an epitope of SARS-coronavirus nucleocapsid protein. *Cell Res* 2003;13:141–5.
- Chen Z, Pei D, Jiang L, Song Y, Wang J, Wang H, et al. Antigenicity analysis of different regions of the severe acute respiratory syndrome coronavirus nucleocapsid protein. *Clin Chem* 2004;50:988–95.
- Pollock RR, Teillaud JL, Scharff MD. Monoclonal antibodies: a powerful tool for selecting and analyzing mutations in antigens and antibodies. *Annu Rev Microbiol* 1984;38:389–417.
- Yewdell JW, Gerhard W. Antigenic characterization of viruses by monoclonal antibodies. *Annu Rev Microbiol* 1981;35:185–206.
- Che XY, Qiu LW, Pan YX, Wen K, Hao W, Zhang LY, et al. Sensitive and specific monoclonal antibody-based capture enzyme immunoassay for detection of nucleocapsid antigen in sera from patients with severe acute respiratory syndrome. *J Clin Microbiol* 2004;42:2629–35.
- Che XY, Qiu LW, Pan YX, Xu H, Hao W, Liao ZY, et al. Rapid and efficient preparation of monoclonal antibodies against SARS-associated coronavirus nucleocapsid protein by immunizing mice. *Di Yi Jun Yi Da Xue Xue Bao* 2003;23:640–2.
- Boder ET, Wittrup KD. Yeast surface display for directed evolution of protein expression, affinity, and stability. *Methods Enzymol* 2000;328:430–44.
- Wen K, Mei YB, Qiu LW, Liao ZY, Yuen KY, Che XY. Preparation and characterization of monoclonal antibodies against S1 domain at N-terminal residues 249 to 667 of SARS-associated coronavirus S1 protein. *Di Yi Jun Yi Da Xue Xue Bao* 2004;24:1–6.
- Ellgaard L, Helenius A. Quality control in the endoplasmic reticulum. *Nat Rev Mol Cell Biol* 2003;4:181–91.
- Shusta EV, Raines RT, Pluckthun A, Wittrup KD. Increasing the

- secretory capacity of *Saccharomyces cerevisiae* for production of single-chain antibody fragments. *Nat Biotechnol* 1998;16:773–7.
34. Mischo A, Wadle A, Watzig K, Jager D, Stockert E, Santiago D, et al. Recombinant antigen expression on yeast surface (RAYS) for the detection of serological immune responses in cancer patients. *Cancer Immun* 2003;3:5–15.
 35. Johns TG, Adams TE, Cochran JR, Hall NE, Hoyne PA, Olsen MJ, et al. Identification of the epitope for the epidermal growth factor receptor-specific monoclonal antibody 806 reveals that it preferentially recognizes an untethered form of the receptor. *J Biol Chem* 2004;279:30375–84.
 36. Cochran JR, Kim YS, Olsen MJ, Bhandari R, Witttrup KD. Domain-level antibody epitope mapping through yeast surface display of epidermal growth factor receptor fragments. *J Immunol Methods* 2004;287:147–58.
 37. Sahin U, Tureci O, Pfreundschuh M. Serological identification of human tumor antigens. *Curr Opin Immunol* 1997;9:709–16.
 38. Sun ZF, Meng XJ. Antigenic cross-reactivity between the nucleocapsid protein of severe acute respiratory syndrome (SARS) coronavirus and polyclonal antisera of antigenic group I animal coronaviruses: implication for SARS diagnosis. *J Clin Microbiol* 2004;42:2351–2.
 39. Woo PC, Lau SK, Wong BH, Chan KH, Hui WT, Kwan GS, et al. False-positive results in a recombinant severe acute respiratory syndrome-associated coronavirus (SARS-CoV) nucleocapsid enzyme-linked immunosorbent assay due to HCoV-OC43 and HCoV-229E rectified by Western blotting with recombinant SARS-CoV spike polypeptide. *J Clin Microbiol* 2004;42:5885–8.
 40. Liu X, Shi Y, Li P, Li L, Yi Y, Ma Q, et al. Profile of antibodies to the nucleocapsid protein of the severe acute respiratory syndrome (SARS)-associated coronavirus in probable SARS patients. *Clin Diagn Lab Immunol* 2004;11:227–8.
 41. ter Meulen J, Bakker AB, van den Brink EN, Weverling GJ, Martina BE, Haagmans BL, et al. Human monoclonal antibody as prophylaxis for SARS coronavirus infection in ferrets. *Lancet* 2004;363:2139–41.
 42. Traggiai E, Becker S, Subbarao K, Kolesnikova L, Uematsu Y, Gismondo MR, et al. An efficient method to make human monoclonal antibodies from memory B cells: potent neutralization of SARS coronavirus. *Nat Med* 2004;10:871–5.
 43. Zhao P, Cao J, Zhao LJ, Qin ZL, Ke JS, Pan W, et al. Immune responses against SARS-coronavirus nucleocapsid protein induced by DNA vaccine. *Virology* 2005;331:128–35.
 44. Xiong S, Wang YF, Zhang MY, Liu XJ, Zhang CH, Liu SS, et al. Immunogenicity of SARS inactivated vaccine in BALB/c mice. *Immunol Lett* 2004;95:139–43.
 45. Kim TW, Lee JH, Hung CF, Peng S, Roden R, Wang MC, et al. Generation and characterization of DNA vaccines targeting the nucleocapsid protein of severe acute respiratory syndrome coronavirus. *J Virol* 2004;78:4638–45.
 46. Skowronski DM, Astell C, Brunham RC, Low DE, Petric M, Roper RL, et al. Severe acute respiratory syndrome (SARS): a year in review. *Annu Rev Med* 2005;56:357–81.
 47. Lai MM. SARS virus: the beginning of the unraveling of a new coronavirus. *J Biomed Sci* 2003;10:664–75.
 48. Risco C, Anton IM, Enjuanes L, Carrascosa JL. The transmissible gastroenteritis coronavirus contains a spherical core shell consisting of M and N proteins. *J Virol* 1996;70:4773–7.
 49. Rossmann MG, Johnson JE. Icosahedral RNA virus structure. *Annu Rev Biochem* 1989;58:533–73.
 50. Rota PA, Oberste MS, Monroe SS, Nix WA, Campagnoli R, Icenogle JP, et al. Characterization of a novel coronavirus associated with severe acute respiratory syndrome. *Science* 2003;300:1394–9.
 51. Marra MA, Jones SJ, Astell CR, Holt RA, Brooks-Wilson A, Butterfield YS, et al. The genome sequence of the SARS-associated coronavirus. *Science* 2003;300:1399–404.
 52. Huang Q, Yu L, Petros AM, Gunasekera A, Liu Z, Xu N, et al. Structure of the N-terminal RNA-binding domain of the SARS CoV nucleocapsid protein. *Biochemistry* 2004;43:6059–63.
 53. Nelson GW, Stohlman SA, Tahara SM. High affinity interaction between nucleocapsid protein and leader/intergenic sequence of mouse hepatitis virus RNA. *J Gen Virol* 2000;81:181–8.